 https://doi.org/10.3311/PPci.20845

Periodica Polytechnica Civil Engineering, 67(1), pp. 80–92, 2023

Investigation of Pore and Filling Material Bond in Filled Travertine Used as a Building Material

Sevgi Çetintaş[1*]

[1] Vocational School of Technical Sciences, Akdeniz University, Dumlupınar Boulevard, 07058, Antalya, Turkey
[*] Corresponding author, e-mail: scetintas@akdeniz.edu.tr

Received: 18 July 2022, Accepted: 27 September 2022, Published online: 04 October 2022

Abstract

Pores, voids, and cracks reduce the strength and economic value of travertine and limits its use. When used as a building material, travertine is often filled to increase its strength and extend its service life. The present experimental study investigates the bond between the pore filler in cement-based filling materials and travertine. For the purpose of the study, five travertine samples were filled with a cement-based filling material. A polarized microscope was used for the mineralogical-petrographic characterization of the travertines, while an image analysis software program (CLEMEX) was used to determine pore size and the number of travertines. A mercury intrusion porosimetry (MIP) technique was used to determine the size and the distribution of pores in the travertine, while the pore filling was identified and characterized using scanning electron microscopy (SEM) and energy-dispersive X-ray spectroscopy (EDX). The pore structure, the bonding of the filler with the pore and the filler performance were then discussed. There was no gap between the pore filling and the Noche travertine sample. The best pore-fill-travertine bond was formed. An opening at the border of the pore filling and the travertine was visible in the Yellow travertine sample. Shrinkages and collapses were noted in the applied filling process, and filing shrinkage was also noted in the Red, Silver and Light travertine samples, preventing the establishment of a healthy connection between the pore filling and the travertine.

Keywords

travertine, filling material, pore, SEM

1 Introduction

Travertine is often used as a building material due to the ease of cutting and processing, and has seen frequent use in monuments, as a cladding for modern buildings and for artistic works. In recent years, travertines of different colors have been used in the Colosseum in Rome, in the ancient cities of Hierapolis, Laodicea and Tripoli in Denizli, and in Anıtkabir in Ankara [1, 2]. Travertine is generally cream in color, although colored travertine deposits (yellow, gray, pink, red and brown) have recently been discovered [3–6], expanding its use different areas.

Travertine is a chemically precipitated continental limestone that is formed around seepages and springs, and along streams and rivers, and occasionally in lakes. It consists of calcite or aragonite, has low-to-moderate intercrystalline porosity, and often has high moldic or framework porosity within the vadose zone [7, 8]. Due to its travertine formation characteristics, the pores are characteristic of all travertines [9]. Its textural diversity can be attributed to the variations in its pore and sedimentary structural features [10]. Pores, voids and cracks reduce the strength and economic value of travertine and limit its use, and so it is of great importance to define the porosity of travertine, being the ratio of the void volume to the total volume. That said, it is not easy to quantify porosity [11], although visual and laboratory methods have been suggested. The Saturation-buoyancy method, based on Archimedes' principle (ISRM 2007), is the most common approach to pore calculations [12], while another common method is the mercury intrusion pore (MIP) measurement approach, which is used to determine the pore size distribution curves of porous stones, as well as the porosity value [13–15]. Porosity has also been measured using nitrogen adsorption and helium expansion porosimetry methods [16–18]. In the petrographic image analysis method, porosity is measured through the dot counting of visible pores on a thin section using image analysis software, thus determining total

Cite this article as: Çetintaş, S. "Investigation of Pore and Filling Material Bond in Filled Travertine Used as a Building Material", Periodica Polytechnica Civil Engineering, 67(1), pp. 80–92, 2023. https://doi.org/10.3311/PPci.20845

porosity, and the size and shape of pores [19, 20]. Porosity, pore spacing and pore morphology, on the other hand, can be determined using digital image analysis techniques at different magnifications from optical or backscattered electron images [21]. All the above methods have advantages and disadvantages, and so it is necessary to use them together to determine the porosity of travertine. Filling the pores in travertine turn it into a strong building material with an extended service life against atmospheric and biological effects [22, 23]. The available filling approaches include epoxy, polyester, ultraviolet, mastic, cement and surface-protective materials, among which cement is today the most common method for travertine tiles. There is no standardized procedure for cement filling among travertine companies – each uses filling materials comprising different ratios of cement, calcite, stuff and coloring agents, depending on the structure and color of the stone. After filling, the material is dried, and the travertine surface is polished after the appropriate curing time. In recent years, researchers have come up with alternative filling materials to improve the appearance and the physical and mechanical properties of travertine, and new repair and application techniques have achieved satisfactory results in the improvement of production quality [24]. Acar's [25] study of materials for the repair and filling of stones identified some important points that should be considered in practice, and examined the economic dimension of repair-filling applications. Demirdag and Gündüz [26] reported a 30% increase in the uniaxial compressive strength of travertine after cement filling. Demirdag [27] used Stuff (ST) and Polyacrylamide (PA) additives in different proportions for filling, and examined the collapse of the filling material from the pores, the optimum curing time, and the change in the physical and mechanical properties of filled travertines, and also conducted laboratory experiments to better understand the effect of freeze-thaw and thermal shock cycles in filled and unfilled travertine samples [28]. Çobanoğlu and Çelik [29] used travertine powder instead of calcite in four different ratios for filling, and determined that the physical properties of the filled travertine plates changed.

A review of previous literature revealed studies in which different mixing ratios of filling material were assessed, as well as the use of different polymer or cement-based materials, aiming to determine the physical and mechanical properties of travertines. To date, however, there have been no studies evaluating the filling of travertine pores with cement- and polymer-based materials and assessing the compatibility and performance of the filler with the pore. While cement-based fillings are preferred over resin and polyester fillings, they have some disadvantages related to the cement in their structure. During curing, shrinkage, cracking collapse or displacement of the filling occurs, and the cracking and dislocation of the filling can also be observed during the polishing process after curing, and also during its use as a building material. For this reason, it is of great importance to examine the relationship between the pore and the filling material in travertine. The present study investigates the bond between the pore filling materials and the travertine in five travertine samples with different pore distributions obtained from different regions after filling with a cement-based filling material. Petrographic image analysis and mercury porosimetry methods were used to determine the size and distribution of pores. A cement-based filling material was prepared and applied, with filling and polishing operations carried out at fixed machine parameters. A scanning electron microscope (SEM) analysis was used to determine the bonding relationship between the pore filling and the travertine, and the gaps between the filling and the travertine, and the level of change were discussed.

2 Materials and method

2.1 Materials

For the study, five types of travertine that are widely used in interior cladding, exterior cladding and floor tile applications were obtained from quarries in Denizli (Honaz), Kütahya (Altıntaş) and Afyonkarahisar (Emirdağ), Turkey (Fig. 1) [30].

Travertines come in different colors: Denizli travertines are creamy Yellow and dark; Silver travertine is gray; and Red travertine is Red and pink. The color of the travertine depends on the physicochemical properties of the water in the location: Red comes from water-soluble iron, Yellow from sulfur, and white or gray from calcium ions [31]. The chemical composition of the travertine samples assessed in the study are presented in Table 1.

Fig. 1 Location map of travertine samples a) Denizli (Honaz), b) Kütahya (Altıntaş), c) Afyonkarahisar (Emirdağ) [30]

Table 1 Chemical composition of the travertine samples (LOI: Loss of ignition)

Oxides	Red Trav	Silver Trav	Noche Trav	Yellow Trav	Light Trav
SiO_2	1.16	1.07	0.95	0.40	0.26
Al_2O_3	0.14	0.12	0.15	0.95	0.08
Fe_2O_3	0.44	0.27	0.06	0.30	0.04
MgO	0.30	0.21	1.60	0.44	0.42
CaO	54.70	54.20	53.50	54.30	54.10
Na_2O	0.02	0.06	0.03	0.03	0.05
K_2O	0.05	0.04	0.02	0.22	0.01
MnO	0.07	0.05	0.02	0.01	0.01
LOI	43.12	43.98	43.67	43.35	45.03

2.2 Method

2.2.1 Filling

The filling process was carried out at a marble factory in Afyonkarahisar, where White Portland cement (CEM I 52.5 R), stuff and paint were used as the filling material. The cement had an average whiteness of 85.2% and a 28-day compressive strength of 60 MPa, which can be considered high. The chemical composition of WPC is presented in Table 2. Stuff is an inorganic material and it is a kind of powder filling material consisting of a triple mixture of aluminum silicate, melamine sulfate and salicylic acid. This type of additive reacts with cement to set early and increases cohesion and strength values at low temperatures.

To prepare the filling material, the WPC, paint and stuff were first dry mixed in a tank for 30 minutes (Fig. 2). The travertine sample surfaces were wetted and fed onto the band of the filling machine at a band speed of 2–2.5 m/min without no gaps left between the samples. In the filling process, the first and second heads are wet (water/cement ratio approx. 0.20), the third and fourth head are semi dry (water/cement ratio approx. 0.05) and the final second hoop is dry (Fig. 2). The filling material was fed to the hoop, rotating at 1500 rpm, with the help of a shovel, and the filled samples were then removed from the machine. The samples were stacked with their filled surfaces facing each other and allowed to dry for two days. After drying, all samples were polished using a computer-controlled polishing machine consisting of two calibers and four abrasive heads (rotation speed 500 rpm).

2.2.2 Analytical applications

The elements in the samples and the cement were determined using a Rigaku-brand X-ray fluorescence spectrometry (XRF- Rigaku) device. During the preparation of the samples for chemical analysis, glass tablets were prepared by melting a 1/10 by weight sample/Li2B4O7 mixture in platinum crucibles in a melter, and semi-quantitative percent by weight chemical analysis results were obtained.

Table 2 Chemical composition of the White Portland Cement (LOI: Loss of ignition)

Oxides	%
CaO	64.5
SiO_2	23.4
Fe_2O_3	0.30
MgO	1.28
Al_2O_3	4.22
SO_3	3.05
K_2O	0.38
Na_2O	0.44
LOI	2.43

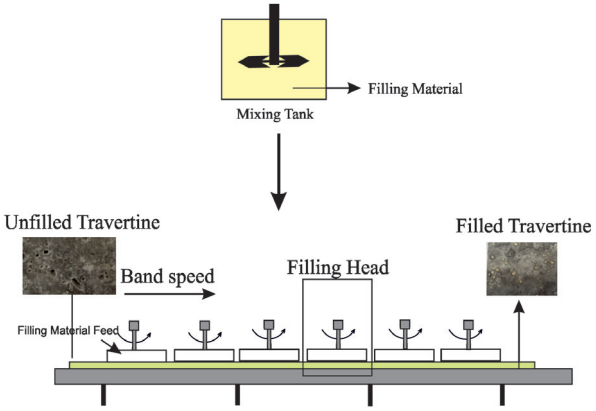

Fig. 2 Filling application flowchart

Mercury intrusion porosimetry (MIP) is commonly used to characterize the structure and distribution of pores in stone [32, 33]. The travertine porosity and pore size distribution was ascertained in the present study using an Autopore IV 9500 Micromeritics mercury porosimetry.

A polarizing optical microscope was then used to determine the mineralogical and petrographic characteristics of the samples, for which a thin section of each sample was prepared. The mineral compositions and morphological properties of the sample were examined using a Nikon Eclipse 2V100 POL polarized light microscope. It is of vital importance to determine the distribution and size of the pores in travertine before filling, and so the pore distribution dimensions were measured using a computer image processing system (CLEMEX) with a polarizing light microscope. The minerals were analyzed chemically using an LEO - 1431-VP model scanning electron microscope (SEM) to determine the filling performance of the samples and to explain the interaction between the filler and the pores.

3 Results and discussion

3.1 Mineralogical and petrographical characteristics of the travertines

The distribution and size of pores may cause filling collapses or fractures in the surface of travertine during filling, or when it is used as a building material. It is of great importance, therefore, to identify the minerals contained within the travertine and the distribution and size of the pores. Fig. 3 shows the samples and the thin sections. Calcite was the main mineral in all samples. The Noche, Yellow, and Light travertine samples from Denizli had an average grain size of 6.14 µm, 31.3 µm and 7.78 µm, respectively, while the size and distribution of the pores were irregular. The Denizli samples were generally composed of micritic and sparicalcite grains. Sparicalcite crystals grew as radial crystals on the micritic ground. The samples had a small amount of melting voids (Fig. 3(h)–(j).

The Silver travertine sample from Afyonkarahisar (Emirdağ) was composed mainly of calcite and had an average calcite grain size of 10.2 µm and smaller melting gaps than the Denizli samples. Silver travertines contain micrite and sparicalcite minerals, while micritic calcite crystals were uniformly distributed throughout the Red travertine from Kütahya (Altıntaş) (Fig. 3(f)), which had an average grain size of 15.8 µm. The Red travertine also had the smallest pore diameter (91 µm) and a sparse pore distribution, and the lowest number of pores (8.4%), followed by the Light (12.1%), Yellow (13.1%), Silver (13.3%) and Noche samples (13.8%). According to the CLEMEX data, the particle size and pore diameter varied widely across the samples (Table 3), which is to be expected given the formation processes of travertine. Pore structure negatively affects the physical and mechanical properties of travertine [34], and so the shape and size of pores should be determined prior to using travertine as a building material for structures with an extended lifespan. The performance of the filler and the interactions between the pore and the filler are key in addition to pore sizes.

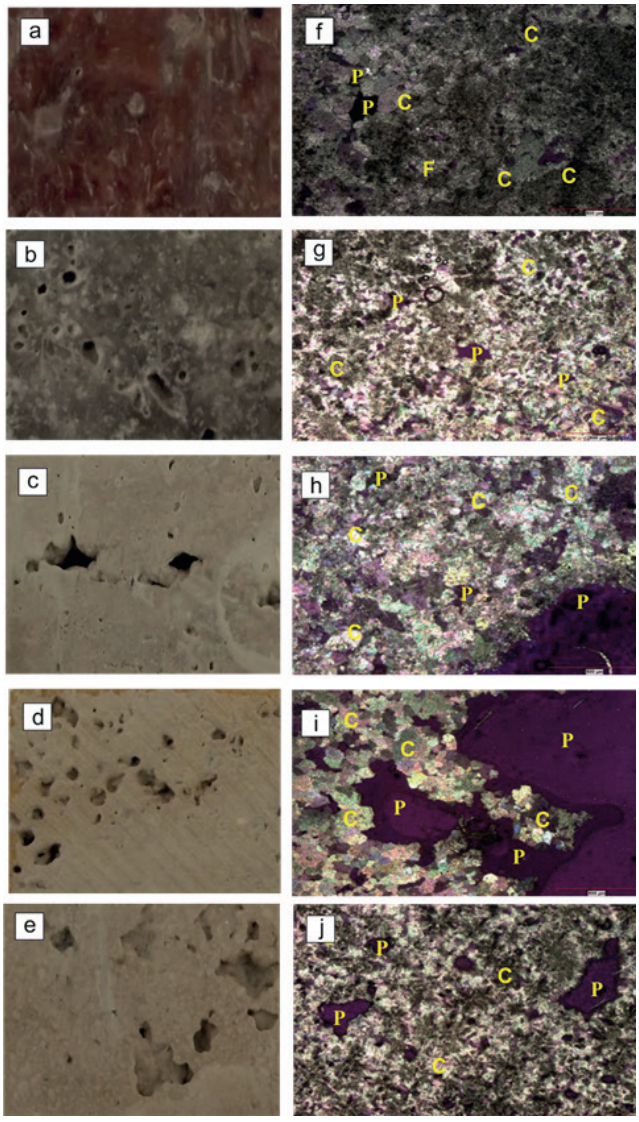

Fig. 3 Macroscopic images a) Red travertine, b) Silver travertine, c) Noche travertine, d) Yellow travertine, e) Light travertine. Mineralogical-petrographic photomicrographs (f) Red travertine, g) Silver travertine, h) Noche travertine, i) Yellow travertine j) Light travertine C: calcite, P: pore

3.2 Pore size distribution (MIP) of travertines

Porosity is a physical property that is affected the formation processes of travertine, and the physical and mechanical properties of travertine, likewise, depend on the formation

Table 3 Calcite particle size and pore diameter

	Pore Degree	Calcite Particle size (µm)			Pore diameter (µm)		
	%	Min.	Max.	Avg.	Min.	Max.	Avg.
Red Travertine	8.4	1.9	193.1	15.8	13.9	745	91
Silver Travertine	13.3	1.9	86.2	10.2	16.6	417.0	150.4
Noche Travertine	13.8	1.9	40.1	6.14	82.8	124.6	546.9
Yellow Travertine	13.1	1.9	244.3	31.3	61.3	2450.4	500.0
Light Travertine	12.1	1.9	59.4	7.78	41.8	1828.0	417.7

process. The greater the porosity and the pore network, the lower the strength and the higher the degradation in travertine. Porous structures are exposed to different environmental factors (relative humidity and water permeability) throughout their lifetime and cracks can occur as a result of the deterioration of intergranular bonds in the rock under the effect of water pressure. As a result, the mechanical properties of the rocks decreases and their strength decreases in time [35–38].

Filling methods are used to strengthen travertines and to increase their lifespans, while pore distribution should be determined to understand the performance of the filler. Mercury intrusion porosimetry (MIP) was used to determine the size and distribution of pores in the travertine samples. The Mercury porosimetry results of the travertine samples are presented in Table 4.

The Silver travertine had the largest average pore diameter (0.22 μm), followed by the Red (0.16 μm), Yellow (0.09 μm), Noche and Light travertine (0.03 μm) samples. The Silver, Red, Yellow, Light, and Noche travertines had median pore diameters of 0.11, 0.08, 0.04, 0.02 and 0.01 μm, respectively. The average pore diameters were different in volume, being 0.42, 0.29, 0.17, 0.09 and 0.05 μm (in volume) in the Silver, Red, Yellow, Noche and Light travertines, respectively. The total pore areas were different from the pore diameters, with the highest and lowest pore areas noted in the Noche and Silver travertines, respectively. Although all samples had about the same apparent density, their porosity ranged from 1.98% to 3.65% (Table 4).

Fig. 4 shows the pore size distribution curves of the samples, in which the pore distribution curve of the Red travertine can be seen to have a bimodal distribution in the range of 0.03 μm to 5 μm, while the Silver travertine sample had a pore size distribution of 0.02 μm to 6 μm; the Noche travertine sample had a pore size distribution of 0.004 μm to 10 μm; the Yellow travertine sample had a pore size distribution of 0.01 μm to 9 μm; and the Light travertine sample had a pore size distribution of 0.008 μm to 4 μm. The results revealed the samples to have irregular and different pore size distributions to which we assigned classifications. (<0.1 μm; 0.1–1 μm; >1 μm). The Light travertine sample had the highest pore size distribution (58.73%), whereas the Silver travertine sample had the lowest pore size distribution (10.99%). The Silver travertine sample had the highest pore size distribution, whereas the Light travertine sample had the lowest pore size distribution in the range of 0.1 to 1 μm (28.28%). At >1 μm, the Red and Light travertine samples had the highest and lowest pore size distributions, respectively.

The mercury porosimetry analysis revealed different average pore diameters in the samples, and Molina et al. [39], aside from suggesting that mercury porosimetry does not examine the shape of pores as it sees them as cylinders, also claim that the number of small pores are overestimated in mercury porosimetry. Urosevic et al. [40], on the other hand, claim that the stone damage resulting from the scratching of the stone surface by individual crystal grains during polishing could lead to an increase in the pore count, and so the distribution and shape of the pores in travertine, as well as the overlapping of the pore chambers and pore throats, should also be taken into account when identifying pore diameters.

The mercury porosimetry and the image analysis of thin sections revealed different porosity and pore diameter results. Simple linear regression graphs of each parameter were created to determine the relationship between the porosity and pore diameter measurements of the travertines and the mercury porosimetry and image analysis method. When these graphs in Fig. 5(a) are examined, it can be seen that a linear decreasing relationship ($R^2 = 0.73$) with medium correlation exists between CLEMEX and MIP for pore diameter. For porosity, a moderately increasing linear ($R^2 = 0.66$) relationship was noted between CLEMEX and MIP (Fig. 5(b)).

Table 4 MIP results of travertine samples

	Red Travertine	Silver Travertine	Noche Travertine	Yellow Travertine	Light Travertine
Total intrusion volume (mL/g)	0.009	0.012	0.017	0.016	0.015
Median pore diameter (area) (μm)	0.08	0.11	0.01	0.04	0.02
Average pore diameter (4 V/A) (μm)	0.16	0.22	0.03	0.09	0.03
Median pore diameter (Volume) (μm)	0.29	0.42	0.09	0.17	0.05
Bulk density at 0.52 psia (g/mL)	2.198	2.173	2.134	2.164	2.143
Apparent (skeletal) density (g/mL)	2.242	2.231	2.215	2.240	2.214
Total pore area (m^2/g)	0.23	0.215	2.421	0.7	1.752
Porosity (%)	1.983	2.595	3.652	3.399	3.216

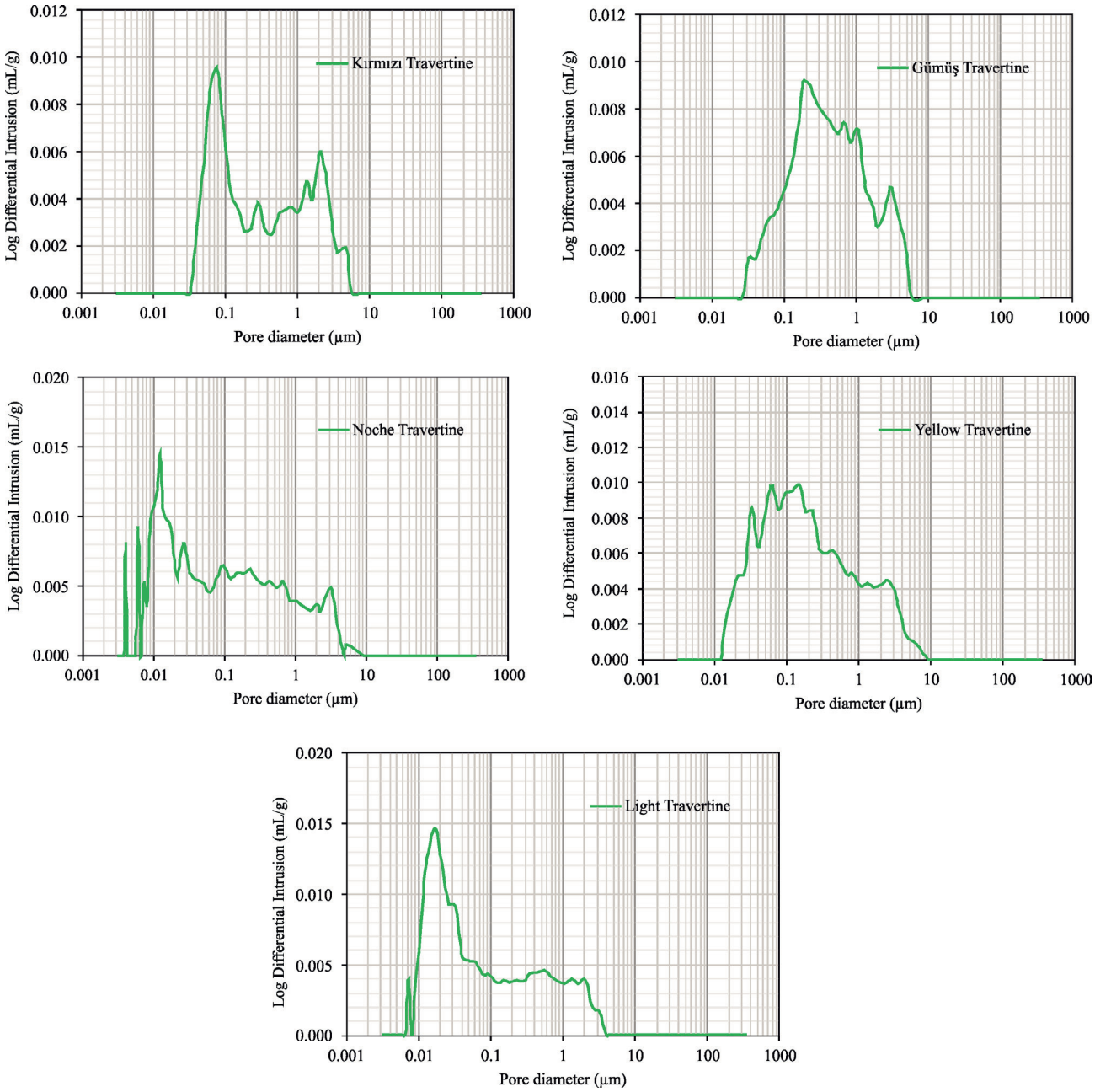

Fig. 4 Pore size distribution of travertine samples

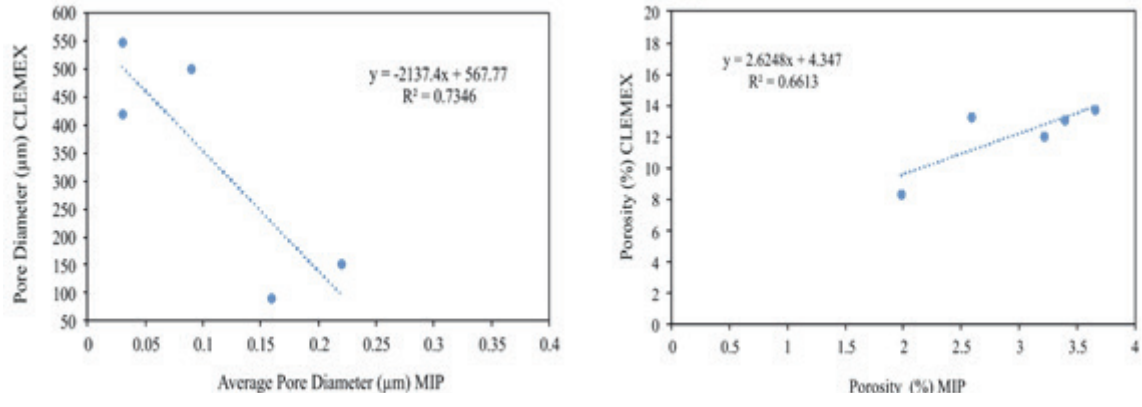

(a) (b)

Fig. 5 Relationship between CLEMEX and MIP a) Pore diameter, b) porosity

Although the correlation rates were not low, they would not be sufficient to estimate different travertine samples as the pores in each sample were of different shapes and sizes. In addition, it does not represent all pores due to the small amount of material used in the mercury porosimeter measurements. This explains the large difference between the obtained measurement data and the pore data obtained from the thin sections.

3.3 SEM analysis following pore filling

In order to better assess the filling process in travertine, the pore filling performance of five different travertine samples filled with the same filling material at a constant belt speed and constant head pressure were analyzed by SEM. Filling curing, filling collapse and cracks occurring in the fill were evaluated considering the bonding relationship between the pore fill and travertine of all samples.

Fig. 6(a) shows the SEM image of the cement pore filling and stone boundary of the Red travertine sample at 100 times magnification, while Fig. 6(b) shows the opening between the pore filling and travertine at 2000 times magnification. Figs. 6(c) and 6(d) show the SEM-EDX spectrum of the filling material and the SEM-EDX spectrum from one point of the travertine, respectively.

In Fig. 6(a), a boundary line can be observed along the filled pore boundary, suggesting a microcrack. When the image of this microcrack area is enlarged, as in Fig. 6(b), an opening at the border of the pore filling and the travertine can be seen. This gap between the fill and travertine was measured to vary between 2.472 µm and 2.810 µm (Fig. 6(b)). In the SEM-EDX micro analysis taken from one point of the filling material, as shown in Fig. 5(c), the C, O, Al, Si, S and Ca elements in the cement content can be determined. Similarly; the Ca, C and O elements representing the calcite crystal can be seen in the point analysis of the travertine sample (Fig. 6(d)). In this travertine example, it can be said that the filling material has not interacted with the travertine, or that the filling has shrunk after drying. Fig. 7(a) shows the SEM micrographs of the Silver travertine sample. The SEM pointed to microcracks with a boundary length of 200 µm. Microcracks are rarely present along the pore boundaries. The length of the

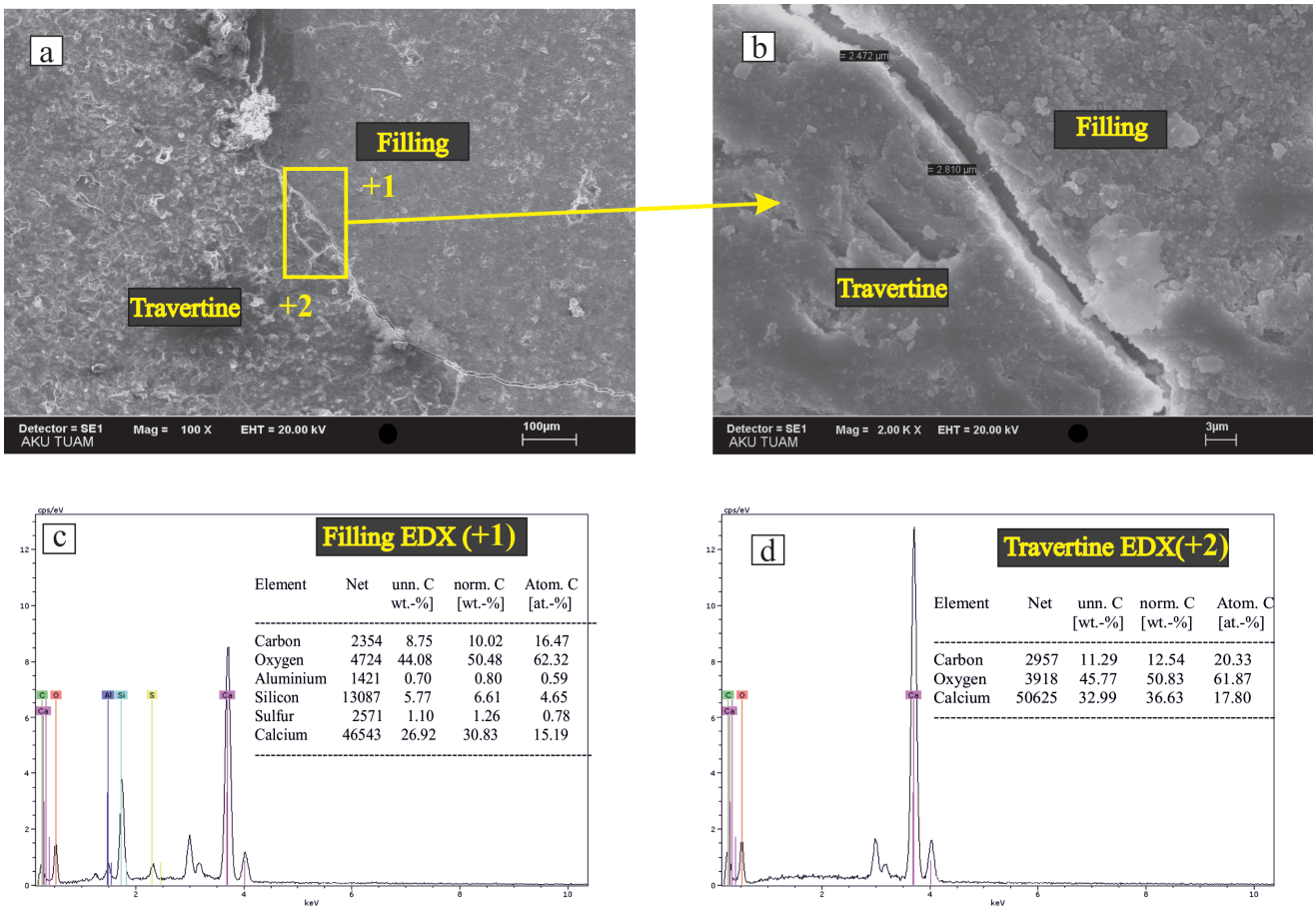

Fig. 6 SEM images of Red Travertine sample a) 100 magnification, b) 2000 magnification, c) Filling material SEM-EDX, d) Travertine SEM-EDX

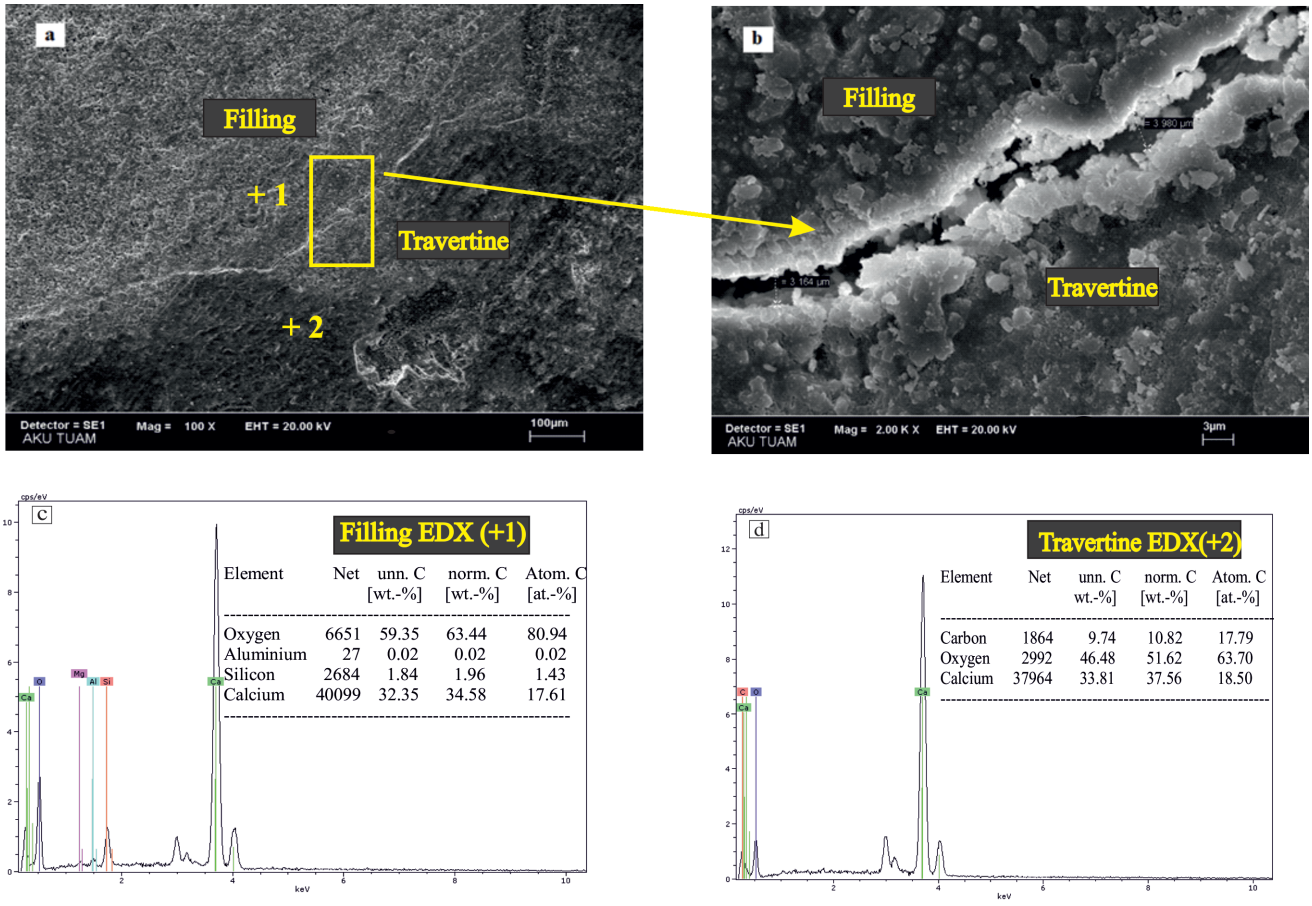

Fig. 7 SEM images of Silver travertine sample a) 100 magnification, b) 2000 magnification, c) Filling material SEM-EDX, d) Travertine SEM-EDX

opening region (the distance between the pore filling and the travertine), defined as a microcrack in Fig. 7(a), varied between 3.164 µm and 3.980 µm (Fig. 7(b)). The density of the particles in this opening showed that the filling material in the pore tended to bond with the travertine. A SEM-EDX analysis of the filling material revealed O, Al, Si and Ca (Fig. 7(c)), while an analysis of the travertine revealed Ca, C and O (Fig. 7(d)).

When Fig. 8(a) of the Noche travertine sample is examined, no opening can be seen, and the filling material and the travertine are integrated. Measuring the microcracks at only one point revealed the distance between the filled pore and the travertine to be between 543.5 nm and 632.8 nm (Fig. 8(b)). In a SEM-EDX point microanalysis, C, O, Si and Ca elements were identified on the fill surface, and Ca, C and O were noted in the travertine (Fig. 8(c) and Fig. 8(d)). The presence of elements on the filling surface is compatible with the presence of elements in the cement, and the same is true for the travertine. The Noche travertine recorded the best pore filling and travertine bonding performance among all the travertine samples.

In the yellow travertine sample, the opening between the pore filling and the travertine boundary is clearly apparent in the SEM image at 100 times magnification, and the filling is connected to the travertine only at one point (Fig. 9(a)). The width of this aperture was measured at approximately 27.92 µm and 26.05 µm at 500 magnification (Fig. 9(b)). This opening is thought to be a result of the filling being insufficient for the pore, or the shrinkage of the filling after curing. As noted in literature, fillers are simultaneously exposed to autogenous shrinkage at the beginning of the hydration reaction after placement, and to long-term drying shrinkage as a result of moisture diffusion [41]. The factors affecting drying shrinkage include relative humidity, the water-cement ratio, the cement type and quality, the age and mixing method [42, 43]. This shrinking phenomenon confirms this by causing a volume change in the material, causing cracks and/or opening in the prefabricated joint.

In the SEM-EDX point microanalysis of the travertine sample, Ca, C and O elements representing the calcite crystal were detected (Fig. 9(c)). In the point analysis of the filling material, C, O, Al, Si and Ca elements representing

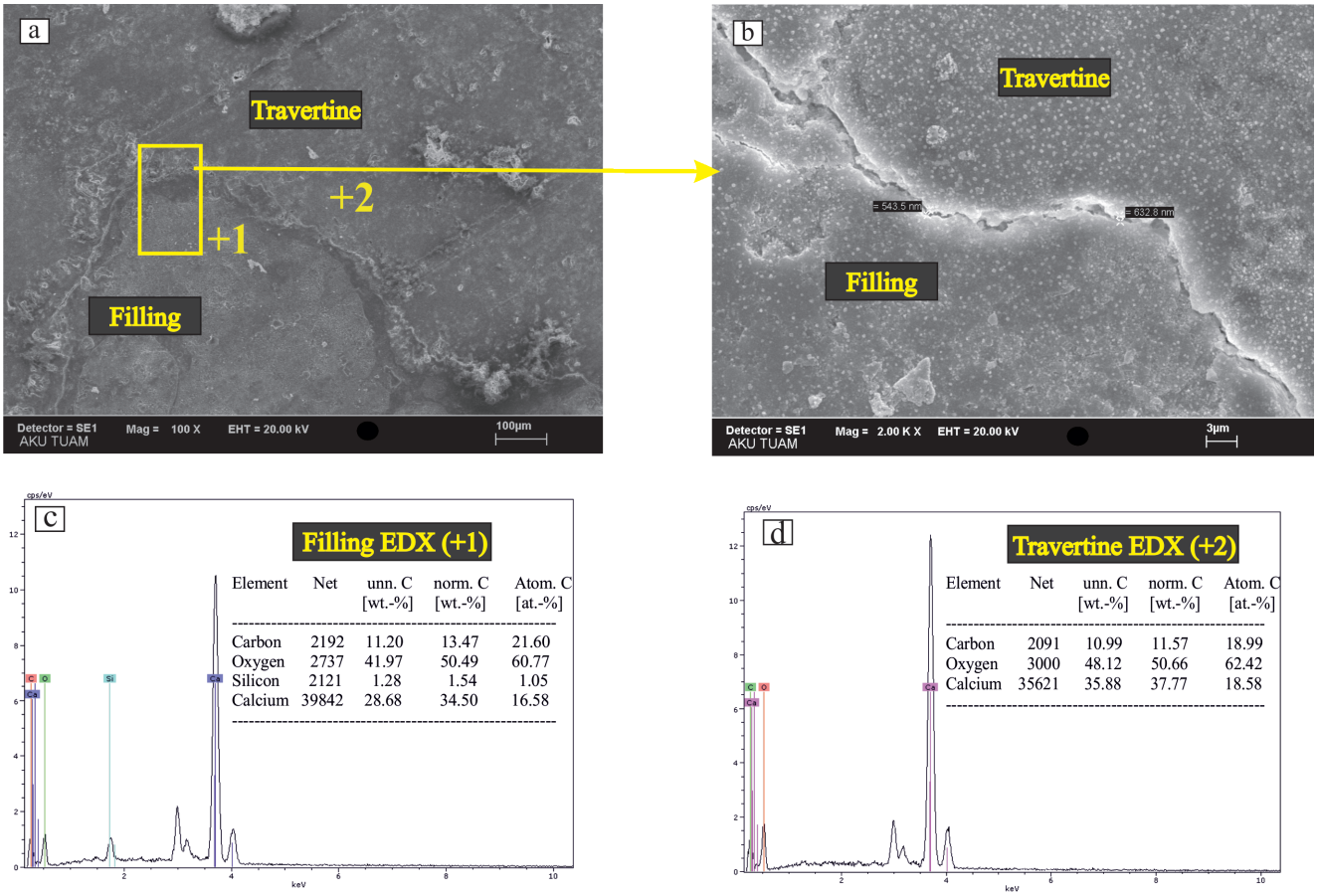

Fig. 8 SEM images of Noche Travertine sample a) 100 magnification, b) 2000 magnification, c) Fill SEM-EDX, d) Travertine SEM-EDX

the cement content were found (Fig. 9(d)). A SEM analysis of the Light travertine sample revealed openings at the fill-travertine boundary that continued along the pore-travertine boundary (Fig. 10(a)). The gap decreased at some points along the pore border, with an aperture width ranging from 7.289 µm to 8.490 µm (Fig. 10(b)). Although traces of ettringite with characteristic shrinkage cracks were found at the travertine-filling interface during curing, the travertine and the filler did not combine well (Fig. 10(b)). A point SEM-EDX analysis revealed C, O, Si and Ca in the filling material (Fig. 10(c)), while an analysis of the travertine revealed Ca, C and O (Fig. 10(d)). The openings at the porous travertine border will lead these fillings to wear and fall in a short time, resulting in reduced strength and a shortened service life.

A microanalysis revealed different tendencies in the fillings applied to each travertine sample. Many parameters can affect the performance of the filling process, making the process complex. Although the machine parameters were kept constant, it was clear that there were still parameters affecting the filling performance, such as pore distribution, size and the sample amount. Both the pore diameter and mercury porosimetry measurements confirm this. When travertines are highly porous, it is difficult to fill the voids resulting in dense filling collapses, which we believe was the cause of the microcracks. In addition, as stated in a previous study, if the fluidity of the filling material is low, it does not fill the entire pore, leading to filling collapse and fracture [44]. In cement-based filling processes, the application of a filling material fluidity according to the pore structure of the stone can ensure both better filling performance and extend the service life of the filled travertines.

4 Conclusions

The durability of travertine is increase through the filling of the pores with a cement-based filling material. This filling material may occur in the use of travertine as a building material, as filling fall and cracking or collapse and displacement during the filling process. The following results were obtained in an experimental study to determine the pore filling and travertine performance of five different travertine samples filled with a cement-based filling material.

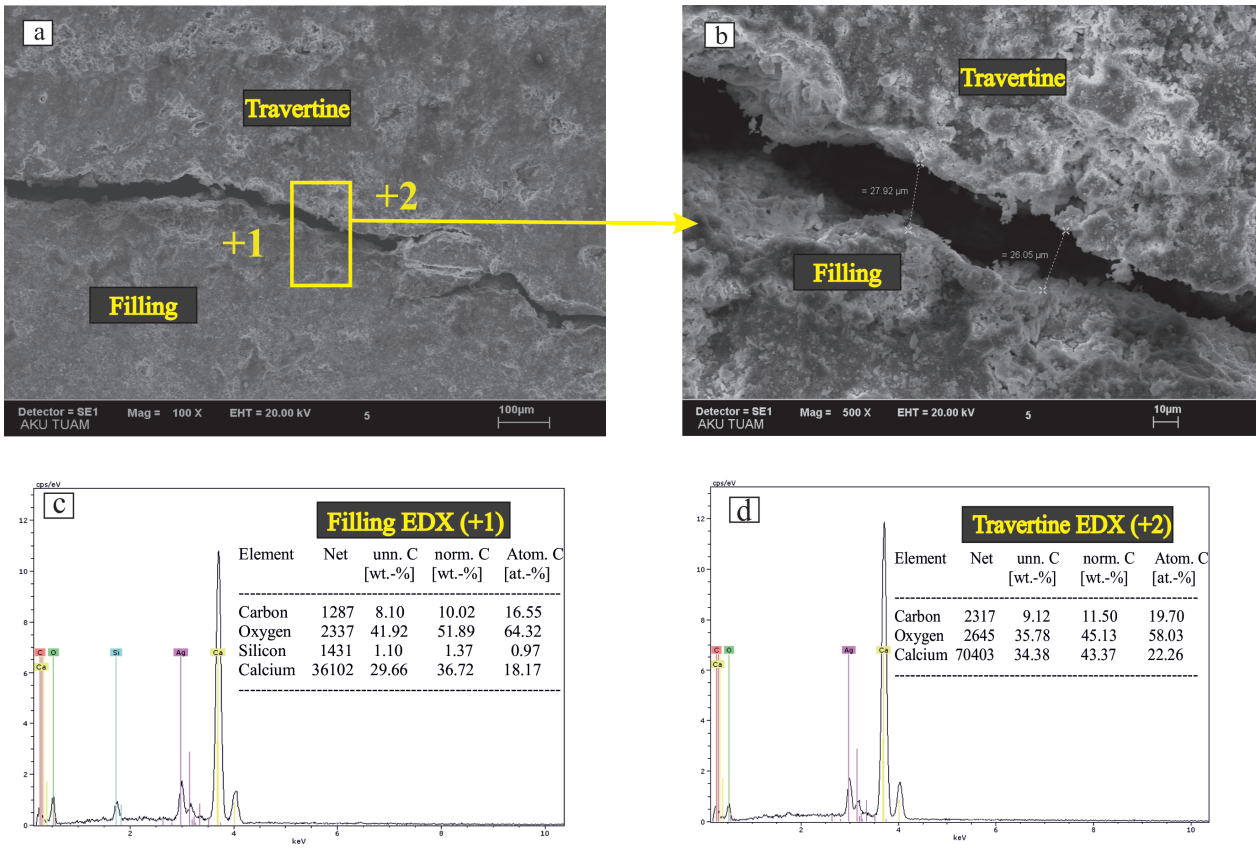

Fig. 9 SEM images of Yellow Travertine sample a) 100 magnification, b) 2000 magnification, c) Fill SEM-EDX, d) Travertine SEM-EDX

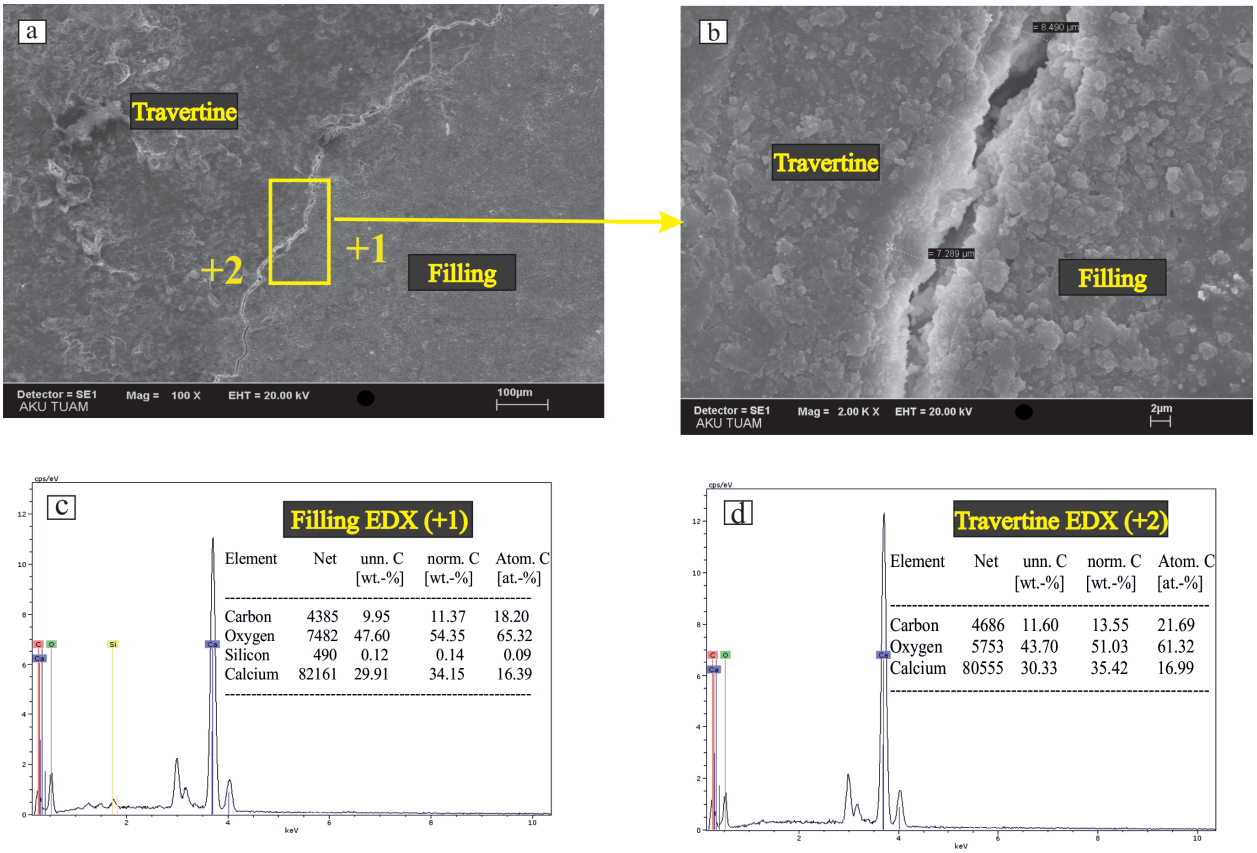

Fig. 10 SEM images of Light Travertine sample a) 100 magnification, b) 2000 magnification, c) Fill SEM-EDX, d) Travertine SEM-EDX

Before the filling process, the mineralogical and petrographic properties of the travertine samples were defined and the pore distributions of the travertine samples were measured using the CLEMEX program. Calcite was the main mineral in all the travertine samples. It was observed that the pore distribution of the samples obtained from the Denizli region (Noche, Yellow and Light travertine) was irregular, with different sizes and fewer melting voids. Smaller melting gaps were observed in the Silver travertine obtained from the Afyonkarahisar (Emirdağ) region than in those from the Denizli region. It was determined that the pore diameters in the Red travertine sample obtained from the Kütahya (Altıntaş) region were the smallest (91 µm) of all the samples, and the pore distribution was not very dense. Since pore structure and distribution are of great importance in filling processes, the mercury intrusion porosimetry technique was used to determine the pore sizes and distributions of the travertine samples before the filling process. When the pore size distribution curves of the travertine samples were examined, the Red travertine samples were found to have a pore size distribution in the range of 0.03 µm to 5 µm, while the Silver travertine sample has a pore size distribution in the range of 0.02 µm to 6 µm. The pore size distribution of the Noche travertine was most varied, ranging between 0.004 µm and 10 µm, while the pore size distribution of the Yellow travertine ranged from 0.01 µm to 9 µm, compared to 0.008 µm to 4 µm in the Light travertine. When the measurement results are classified considering the intervals of <0.1 µm, 0.1–1 µm and >1 µm, the Light travertine sample (48.64%) had the highest value in the range of <0.1 µm, while Silver travertine (63.08%) had the highest value in the range of 0.1-1 µm. The highest value in the >1 µm range in the classification belongs to Red travertine (29.87%). These results confirm the high irregularity of pore distributions in the travertine samples.

An analysis of the CLEMEX and MIP results revealed large differences between the data. Although an attempt was made to establish a relationship between CLEMEX and MIP, the most significant difference is that the pore distribution is not in a size that will represent the whole sample, due to the amount of material used in the MIP method.

After filling the travertine samples with the filling material, the pore-filling performance was analyzed by SEM. No gap was identified between the pore filling and the travertine in the Noche travertine sample, which achieved the best pore filling-travertine performance, although the Silver Travertine sample also performed well, with a micro-opening between the pore filling and the travertine of only 200 µm. The density of the particles observed in this micro-aperture reveals the tendency of the filling material and travertine to combine within the pore. The opening at the border of the pore filling and the travertine was clearly apparent in the Yellow travertine, and it was concluded that this was attributable to the fact that the filling was not sufficient for the pore. In the Red and Light travertine samples, an opening suggesting a micro-crack was observed along the travertine border with the pore filling. It was concluded that the filling performance of the aforementioned samples had not been good. The presence of these openings at the border of the pore filling and the travertine that these fillings will decrease due to both atmospheric effects and abrasion in the future, and as a result, the strength of the travertine will decrease and its lifespan will be shortened when used as a construction material.

Acknowledgement

The author would like to thank the Coordinatorship of the Scientific Research Project of Afyon Kocatepe University for its financial support (Project No: 15.MUH.03).

References

[1] Çobanoğlu, İ., Çelik, S. B. "Determination of strength parameters and quality assessment of Denizli travertines (SW Turkey)", Engineering Geology, 129-130, pp. 38–47, 2012. https://doi.org/10.1016/j.enggeo.2012.01.010

[2] Török, A., Licha, T., Simon, K., Siegesmund, S. "Urban and rural limestone weathering; the contribution of dust to black crust formation", Environmental Earth Sciences, 63, pp. 675–693, 2011. https://doi.org/10.1007/s12665-010-0737-6

[3] Pentecost, A. "Travertine", Springer, 2005. ISBN 978-1-4020-3523-4 https://doi.org/10.1007/1-4020-3606-X

[4] Sidraba, I. "Weatherability of Roman travertine", PhD Thesis, Riga Technical University, 2006.

[5] Akın, M. "A quantitative weathering classification system for yellow travertines", Environmental Earth Sciences, 61(1), pp. 47–61, 2010. https://doi.org/10.1007/s12665-009-0319-7

[6] Zalooli, A., Khamehchiyan, M., Nikudel, M. R. "Durability assessment of Gerdoi and red travertines from Azarshahr, East Azerbaijan province, Iran", Bulletin of Engineering Geology and the Environment, 78, pp. 1683–1695, 2019. https://doi.org/10.1007/s10064-018-1249-y

[7] Pedley, H. M. "Classification and environmental models of cool freshwater tufas", Sedimentary Geology, 68, pp. 143–154, 1990. https://doi.org/10.1016/0037-0738(90)90124-C

[8] Vázquez, P., Alonso, F. J., Carrizo, L., Molina, E., Cultrone, G., Blanco, M., Zamora, I. "Evaluation of the petrophysical properties of sedimentary building stones in order to establish quality criteria", Construction and Building Materials, 41, pp. 868–878, 2013. https://doi.org/10.1016/j.conbuildmat.2012.12.026

[9] Andriani, G. F., Walsh, N. "Physical properties and textural parameters of calcarenitic rocks: qualitative and quantitative evaluations", Engineering Geology, 67, pp. 5–15, 2002. https://doi.org/10.1016/S0013-7952(02)00106-0

[10] Török, Á., Vásárhelyi, B. "The influence of fabric and water content on selected rock mechanical parameters of travertine, examples from Hungary", Engineering Geology, 115, pp. 237–245, 2010. https://doi.org/10.1016/j.enggeo.2010.01.005

[11] Zalooli, A., Khamehchiyan, M., Nikudel, M. R. "The quantification of total and effective porosities in travertines using PIA and saturation-buoyancy methods and the implication for strength and durability", Bulletin of Engineering Geology and the Environment, 77, pp. 1739–1751, 2018. https://doi.org/10.1007/s10064-017-1072-x

[12] Brown, E. T. (ed.) "Rock characterization, testing and monitoring", Pergamon Press, 1981. ISBN 9780080273099

[13] Ordóñez, S., Fort, R., García del Cura, M. A. "Pore size distribution and the durability of a porous limestone", Quarterly Journal of Engineering Geology and Hydrogeology, 30, pp. 221–230, 1997. https://doi.org/10.1144/GSL.QJEG.1997.030.P3.04

[14] Benavente, D., García del Cura, M. A., Fort, R., Ordóñez, S. "Durability estimation of porous building stones from pore structure and strength", Engineering Geology, 74, pp. 113–127, 2004. https://doi.org/10.1016/j.enggeo.2004.03.005

[15] Benavente, D., Pla, C. "Effect of pore structure and moisture content on gas diffusion and permeability in porous building stones", Materials and Structures, 51, 21, 2018. https://doi.org/10.1617/s11527-018-1153-8

[16] Whitham, A. G., Sparks, R. S. J. "Pumice", Bulletin of Volcanology, 48, pp. 209–223, 1986. https://doi.org/10.1007/BF01087675

[17] Angeli, M., Benavente, D., Bigas, J.-P., Menéndez, B., Hébert, R., David, C. "Modification of the porous network by salt crystallization in experimentally weathered sedimentary stones", Materials and Structures, 41, pp. 1091–1108, 2008. https://doi.org/10.1617/s11527-007-9308-z

[18] Soete, J., Kleipool, L. M., Claes, H., Claes, S., Hamaekers, H., Kele, S., Özkul, M., Foubert, A., Reijmer, J. J. G., Swennen, R. "Acoustic properties in travertines and their relation to porosity and pore types", Marine and Petroleum Geology, 59, pp. 320–335, 2015. https://doi.org/10.1016/j.marpetgeo.2014.09.004

[19] Lucia, F. J. "Carbonate Reservoir Characterization", Springer, 2007. ISBN 978-3-540-72740-8 https://doi.org/10.1007/978-3-540-72742-2

[20] Berrezueta, E., González-Menéndez, L., Ordóñez-Casado, B., Olaya, P. "Pore network quantification of sandstones under experimental CO2 injection using image analysis", Computers and Geosciences, 77, pp. 97–110, 2015. https://doi.org/10.1016/j.cageo.2015.01.005

[21] Røgen, B., Gommesen, L., Fabricius, I. L. "Grain size distributions of chalk from image analysis of electron micrographs", Computers and Geosciences 27(9), pp. 1071–1080, 2001. https://doi.org/10.1016/S0098-3004(00)00159-X

[22] Sidraba, I. "New materials for conservation of stone monuments in Latvia. Centre for Conservation and Restoration of Stone Materials", Institute of Silicate Materials, Riga Technical University, Azenes 14/24, LV-1048, Riga, Latvia, 2021. [online] Available at: https://citeseerx.ist.psu.edu/viewdoc/download?doi=10.1.1.516.3791&rep=rep1&type=pdf

[23] Isık, E. C., Ozkahraman, H. T. "An economic solution to high quality travertine filling", Construction and Building Materials, 24(12), pp. 2619–2627, 2010. https://doi.org/10.1016/j.conbuildmat.2010.04.066

[24] Pomakis, I., Mecik, A. "Modern kimyasal uygulama işlemleri ile doğal tasların kalitesinin arttırılması" (Increasing the quality of natural stones with modern chemical application processes), Türkiye Taş Dünyası, Taş ve Taş Teknolojileri Dergisi, 22, pp. 92–98, 2001. (in Turkish)

[25] Acar, H. "Doğal taşlarda çatlak tamir ve gözenek dolgu sistemleri" (Crack repair and pore filling systems in natural stones), In: Turkey IV. Marble Symposium, Afyonkarahisar, Turkey, 2003, pp. 415–434. (in Turkish)

[26] Demirdag, S., Gunduz, L. "A numerical analysis for the effect of pore filling applications in travertines on technical parameters of the rock", In: Rockmec'2004 VIIth regional rock mechanics symposium, Sivas, Turkey, Online, 2004.

[27] Demirdag, S. "The effect of using different polymer and cement based materials in pore filling applications on technical parameters of travertine stone", Construction and Building Materials, 23(1), pp. 522–530, 2009. https://doi.org/10.1016/j.conbuildmat.2007.10.019

[28] Demirdag, S. "Effects of freezing–thawing and thermal shock cycles on physical and mechanical properties of filled and unfilled travertines", Construction and Building Materials, 47, pp. 1395–1401, 2013. https://doi.org/10.1016/j.conbuildmat.2013.06.045

[29] Çobanoğlu, İ., Çelik, S. B. "Evaluation of the use of an alternative mixture for pore filling material on travertine slabs", Pamukkale University Journal of Engineering Sciences, 26(8), pp. 1373–1378, 2020. https://doi.org/10.5505/pajes.2020.84584

[30] Mineral Research and Exploration General Directorate "GeoScience" 2022. [map] Available at: http://yerbilimleri.mta.gov.tr/home.aspx [Accessed: 23 September 2022]

[31] Polat, S. "Türkiye'de Traverten Oluşumu, Yayılış Alanı Ve Korunması" (The Formation, Spread Area and Protection of Travertine in Turkey), Marmara Coğrafya Dergisi, 23, pp. 389–428, 2011. (in Turkish)

[32] Benavente, D., Such-Basañez, I., Fernandez-Cortes, A., Pla, C., Cazorla-Amoros, D., Cañaveras, J. C., Sanchez-Moral, S. "Comparative analysis of water condensate porosity using mercury intrusion porosimetry and nitrogen and water adsorption techniques in porous building Stones", Construction and Building Materials, 288, 123–131, 2021. https://doi.org/10.1016/j.conbuildmat.2021.123131

[33] Liu, K., Ostadhassan, M., Cai, J. "Characterizing Pore Size Distributions of Shale", In: Cai, J., Hu, X. (Eds.) Petrophysical Characterization and Fluids Transport in Unconventional Reservoirs, Elsevier, 2019, pp. 3–20. ISBN 978-0-12-816698-7
doi.org/10.1016/B978-0-12-816698-7.00001-2

[34] Akin, M., Özsan, A., Akin, M. "Investigation of the Macro Pore Geometry of Yellow Travertines Using the Shape Parameter Approach", Environmental and Engineering Geoscience, 15(3), pp. 197–209, 2009.
https://doi.org/10.2113/gseegeosci.15.3.197

[35] Rabat, Á, Tomás, R, Cano, M. "Advances in the understanding of the role of degree of saturation and water distribution in mechanical behaviour of calcarenites using magnetic resonance imaging technique", Construction and Building Materials, 303, 124420, 2021.
https://doi.org/10.1016/j.conbuildmat.2021.124420

[36] Rabat, Á, Tomás, R, Cano, M. "Evaluation of mechanical weakening of calcarenite building stones due to environmental relative humidity using the vapour equilibrium technique", Engineering Geology, 278(12), 105849, 2020.
https://doi.org/10.1016/j.enggeo.2020.105849

[37] Rabat, Á, Tomás, R, Cano, M, Miranda, T. "Impact of water on peak and residual shear strength parameters and triaxial deformability of high-porosity building calcarenite stones: Interconnection with their physical and petrological characteristics", Construction and Building Materials, 262, 120789, 2020.
https://doi.org/10.1016/j.conbuildmat.2020.120789

[38] Rabat, Á, Cano, M, Tomás, R. "Effect of water saturation on strength and deformability of building calcarenite stones: Correlations with their physical properties", Construction and Building Materials, 232, 117259, 2020.
https://doi.org/10.1016/j.conbuildmat.2019.117259

[39] Molina, E., Cultrone, G., Sebastián, E., Alonso, F. J., Carrizo, L., Gisbert, J., Buj, O. "The pore system of sedimentary rocks as a key factor in the durability of building materials", Engineering Geology, 118, pp. 110–121, 2011.
https://doi.org/10.1016/j.enggeo.2011.01.008

[40] Urosevic, M., Sebastián-Pardo, E., Cardell, C. "Rough and polished travertine building stone decay evaluated by a marine aerosol ageing test", Construction and Building Materials, 24, pp. 1438–1448, 2010.
https://doi.org/10.1016/j.conbuildmat.2010.01.011

[41] Tazawa, E. "Autogenous shrinkage of concrete", CRC Press, 1999. ISBN 9780429079382
https://doi.org/10.1201/9781482272123

[42] Neville, A. M. "Properties of Concrete", 5th Ed., Longman, 2011. ISBN 9780273755807

[43] Mehta, P. K, Monteiro, P. J. M. "Concrete: Microstructure, Properties, and Materials", 4th Ed., McGraw Hill, 2014. ISBN 9780071797870

[44] Akçakoca, H., Kaya, S., Ören, Ö. "The Quality Control Problems Encountered In Marble - Travertine Factories", Journal of Science and Technology of Dumlupınar Üniversity, 11, pp. 131–142, 2006.